Effect of Iron Catalyst Thickness on Vertically Aligned Carbon Nanotube Forest Straightness for CNT-MEMS

Kellen Moulton[1], Nicholas B. Morrill[2], Adam M. Konneker[2] Brian D. Jensen[1], Richard R. Vanfleet[2], David D. Allred[2], and Robert C. Davis[2]

[1] Mechanical Engineering Department, Brigham Young University, Provo, UT 84602

[2] Department of Physics and Astronomy, Brigham Young University, Provo, UT 84602

E-mail: bdjensen@byu.edu

Abstract. This paper examines the effect of iron catalyst thickness on the straightness of growth of carbon nanotubes for microelectromechanical systems fabricated using the Carbon Nanotube Templated - Microfabrication (CNT-M) process. SEM images of samples grown using various iron catalyst thicknesses show that both good growth straightness and edge definition are achieved using an iron thickness between 7 and 8 nm. Below this thickness, individual CNT's are well-aligned, but the sidewalls of CNT forests formed into posts and long walls are not always straight. Above this thickness, the CNT forest sidewalls are relatively straight, but edge definition is poor, with significantly increased sidewall roughness. CNT growth is also affected by a device's or feature's proximity to other regions of iron. By using an iron catalyst thickness appropriate for straight growth, and by adding borders of iron around features or devices, a designer can greatly improve straightness of growth for CNT-MEMS.

1. Introduction

A novel process for fabricating carbon nanotube microelectromechanical systems has recently been developed. In this process, a 3-dimensional CNT framework is patterned by photolithography and filled by chemical vapor infiltration [1–3]. Using this technique, we have demonstrated operation of MEMS comb drives [2], as well as thermal actuators and bistable mechanisms [1]. This Carbon Nanotube Templated - Microfabrication (CNT-M) process has many potential benefits that differentiate it from other MEMS fabrication processes. Figure 1 shows a device that has been made using the CNT-MEMS process and filled with silicon nitride.

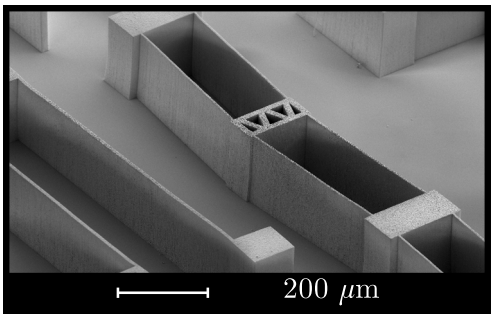

Figure 1. A 220 μm tall CNT-MEMS device that has been filled with silicon nitride. Filling the carbon nanotubes with various materials makes the 3-dimensional framework rigid.

The CNT framework could be filled with many materials compatible with chemical vapor deposition, including some metals. The result is a composite material with CNT fibers and some other matrix material. This would allow a MEMS designer to choose a set of material properties best suited for the application. Note that in most composite materials, the fibers are used only to provide mechanical properties, such as strength, to the matrix material. In CNT-M, the nanotubes not only contribute to the electrical, thermal, and mechanical properties, but also define the shape that the matrix material will take.

Another interesting benefit of this process is that CNT MEMS can be made with very high aspect ratios, comparable to devices made by LIGA [4]. Features that are only a few microns wide can be a few hundred microns tall. In some cases, however, features with very high aspect ratios and poor lateral support, such as posts and long walls, have grown non-straight, resulting in devices with sides that are not vertical. This problem becomes more pronounced as device height increases, as seen in Figure 2. Similarly, Figure 3 shows a comb drive and several beams grown to a height of several hundred micrometers. Thinner beams, as well as thin sections of the comb drive, have grown with non-straight sidewalls in some cases. Improving the straightness of growth would allow for even higher-aspect-ratio devices to be achievable with the CNT-M process.

CNT forests can be grown by chemical vapor deposition (CVD) [5–7]. CVD of carbon nanotubes is accomplished by catalytic decomposition of hydrocarbons, with iron, nickel, and cobalt being the most effective catalysts [8]. This research focuses on the effects of catalyst availability on CNT forests, with iron as the catalyst and ethylene as the hydrocarbon. Prior work studies the effect of pattern density on nanotube growth [9, 10]; this work studies the effect of catalyst thickness.

Previous research has shown that catalyst thickness has several effects on carbon nanotube growth. Thicker layers of iron catalyst result in larger iron particles on which the carbon precipitates,

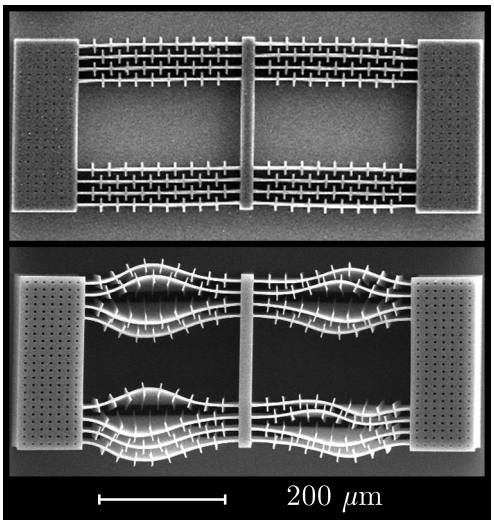

Figure 2. SEM images of devices fabricated from the same pattern. The top image shows a relatively straight device grown to 60 μm tall. The bottom image shows an extreme case of non-straight growth when the same device is grown to 280 μm tall. Both top and bottom are grown with all parameters the same, except for growth time (and hence growth height).

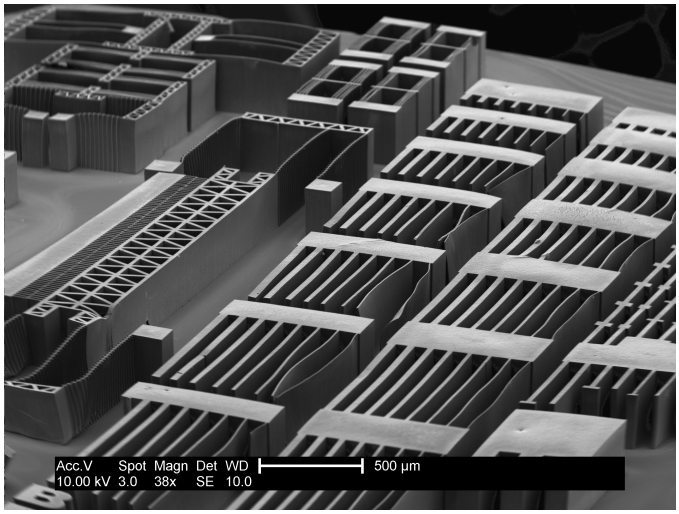

Figure 3. SEM image of a comb drive and several beams. Some thin beams and thin sections have grown with non-straight sidewalls. These devices have been filled with graphitic carbon after nanotube growth.

which results in nanotubes with more walls and higher diameters [11–13]. As catalyst thickness increases, the mechanism of growth transitions from base growth to tip growth [14]. In base growth, nanotubes grow on top of the catalyst, which adheres to the substrate. In tip growth, nanotubes grow between the catalyst particle and the substrate, suspending the catalyst particle in the nanotube forest. Additionally, using relatively thin catalyst layers has been shown to improve alignment of nanotubes within a forest [15]. One possible explanation for this is that thicker catalyst layers result in larger numbers of defects during nanotube growth, producing kinks in the tubes [16, 17].

However, alignment of nanotubes within a forest is different from forest or sidewall straightness.

Within a given CNT forest, the sidewalls may be straight or curved, and the individual nanotubes may vary in a continuum from highly aligned to strongly intertwined. For CNT-M processing, it is desirable to find processing conditions that result in straight walls for the resulting MEMS. Alignment of individual nanotubes does not strongly affect the quality of the CNT-M structures, as long as the intertwining of nanotubes does not result in excessive wall roughness. The purposes of this research are to show the effect of iron catalyst thickness on CNT forest sidewall straightness, find an appropriate range of iron thicknesses for the CNT-M process, better understand what causes non-straight growth, and provide additional guidelines for CNT-M design.

2. Experimental Setup

Two sets of experiments were performed. The purposes of the first set of experiments were to observe the effect of iron catalyst thickness on CNT forest straightness, and to find a suitable range of iron thicknesses for CNT-MEMS. We examined samples with iron catalyst thicknesses of 2, 3, 4, 5, 7.5, 10, and 20 nm. After the first set of experiments, it became clear that a second set of experiments was needed to further examine the range between 7 and 11 nm. The second set of experiments used iron thicknesses of 7, 8, 9, 10, and 11 nm.

Samples were made by the following process (see Figure 4):

(a) Deposit 3 μm SiO_2 onto silicon wafer by PECVD. The oxide is used as a release layer in CNT-M. Deposit a 30 nm layer of alumina on top of the oxide by e-beam evaporation.

(b) Pattern photoresist by photolithography.

(c) Deposit the iron catalyst layer by thermal evaporation.

(d) Lift-off photoresist, leaving behind patterned iron layer.

(e) CVD of carbon nanotubes:

- Place sample in 1 inch tube furnace and heat to 750°C while flowing hydrogen gas (400 SCCM). The purpose of hydrogen is to reduce the iron.
- Flow 99.995% pure ethylene gas (600 SCCM) for desired growth time (typically a few minutes) for CVD of carbon nanotubes.
- At the end of the growth time, stop flow of hydrogen and ethylene, and flow argon (400 SCCM) to flush out hydrogen and ethylene during cooling.

Filling the CNT forests by chemical vapor infiltration and then releasing the devices would complete the CNT-MEMS fabrication process. However, these steps were not necessary to examine forest straightness. Hence, all images shown in this paper, with the exception of Figures 1 and 3, show CNT forests that have not been filled with any other material.

For the first study, samples were grown to a target height of 60 μm tall. For the second study, samples were grown to a target height of 100 μm tall. One reason for varying the growth heights was to find a catalyst thickness that would work well over a range of growth heights, from tens of micrometers to over 100 micrometers. Different heights can be achieved by adjusting the growth time. There is some variability in the process, so using the same growth time does not yield exactly the same height every time. Because forest straightness depends on growth height, samples of each iron thickness were grown within 5% of the target height for comparison. For the first set of

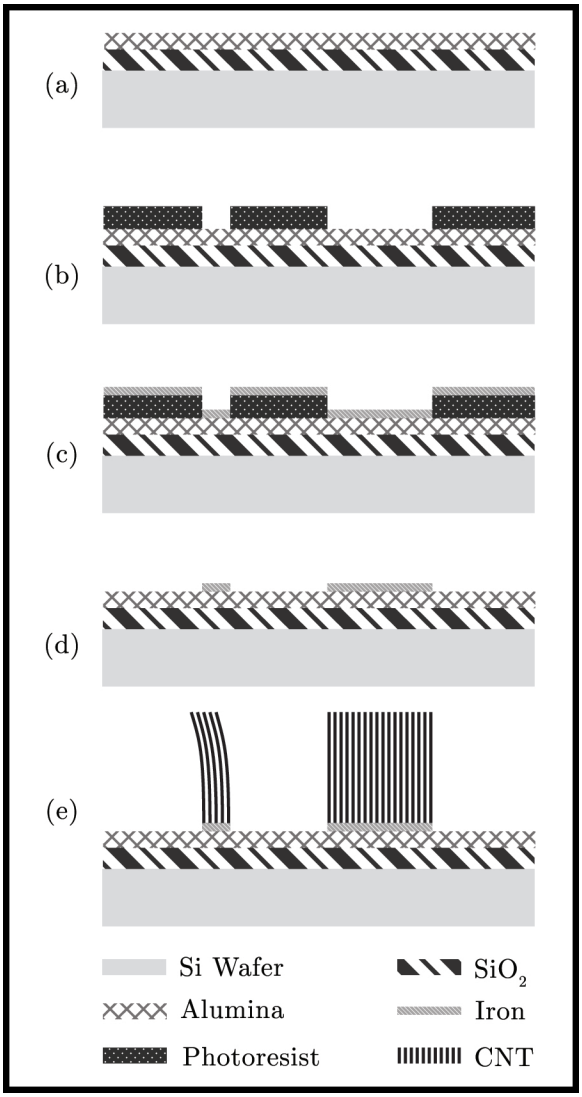

Figure 4. Process used in this study for growing CNT forests (not to scale). (a) Oxide and alumina are deposited onto a silicon wafer. (b) Photoresist is patterned. (c) Iron catalyst layer of desired thickness is deposited. (d) Liftoff leaves behind patterned iron layer. (e) Carbon nanotubes are grown by CVD.

experiments, a total of 34 samples were grown, with at least three samples from each iron thickness. For the second set of experiments, a total of 12 samples were grown, with at least two from each iron thickness.

Scanning electron micrographs that show the top of each sample were used to visually compare the straightness of growth for different catalyst thicknesses. Note that visually observing the top of each sample is useful in identifying the trend for straight growth as well as the general region of straightest growth, but it does not quantify the straightness. As will be seen in the following sections, this method is sufficient for finding the general region of straightest growth and for developing an understanding for what causes nonstraight growth. The results of this study could be used in a future study that quantifies the straightness to gain better precision.

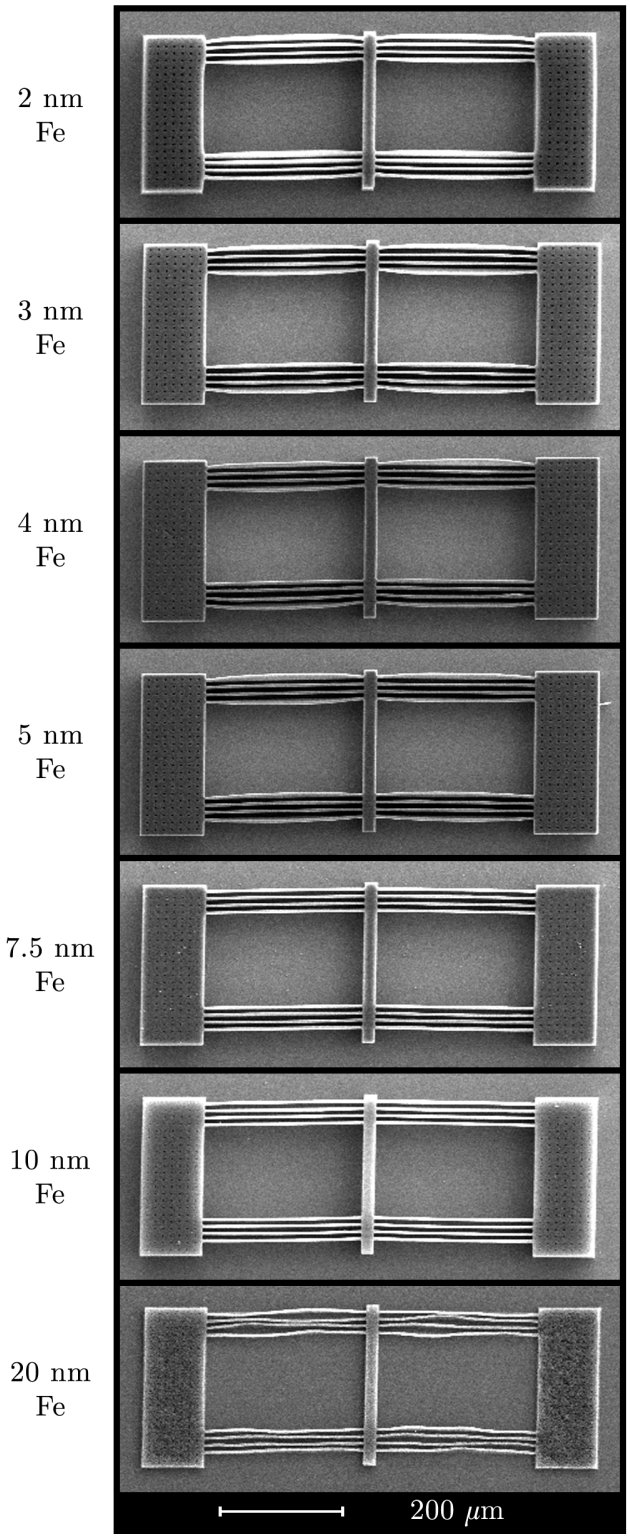

Figure 5. SEM images from the first set of experiments. For samples grown with 2, 3, 4, and 5 nm Fe, the thin walls in the structure shown are clearly non-straight. The samples grown with 7.5 and 10 nm Fe are the straightest. The sample grown with 20 nm Fe has very poorly defined features.

3. Experimental Results

Figure 5 shows SEM images that are typical of the results from the first set of experiments. Only samples within 5% of the target height are directly compared, but the results are consistent with

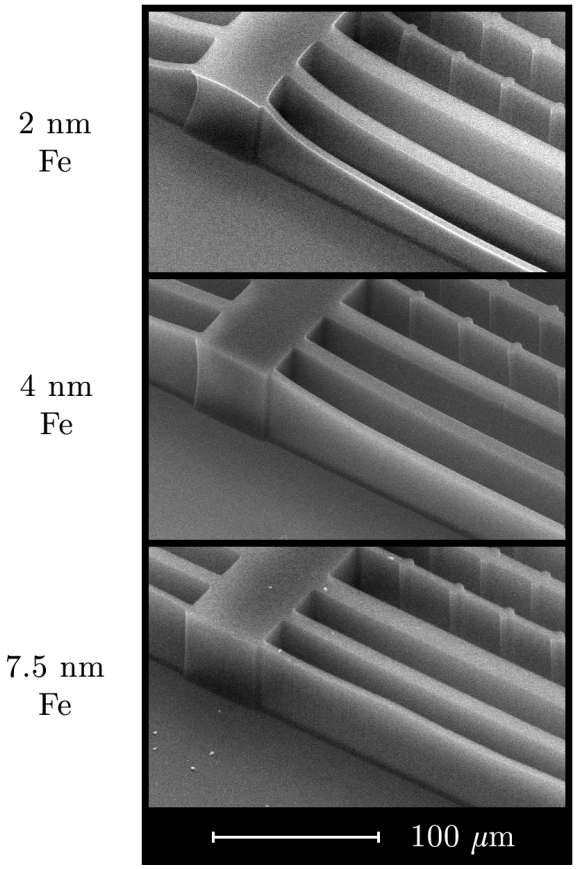

Figure 6. Samples from the first set of experiments that show the difference in growth between edge features that are not in near proximity to other features on all sides, and central features that are. The sample with a 7.5 nm iron layer has enough iron available on the sample to mitigate this effect.

all 34 samples grown. Notice that the samples with 2, 3, 4, and 5 nm of iron are less straight than the samples with 7.5 and 10 nm of iron. The sidewalls for the growths with thin iron also tend to bend outward, away from the other lines. There is no observed difference in straightness between the 7.5 and 10 nm of iron samples. A thicker iron layer yields higher-diameter nanotubes with more walls [11, 12]. The CNTs are also less well-aligned [15]. As evidenced by the image of the 20 nm sample, the lack of CNT alignment may cause the edges of the forest to have poor definition. In this case, the lack of alignment is so severe that the forest no longer retains the original pattern, even at the substrate. This is due to patchy growth, causing the nanotubes to grow in all directions instead of forming a vertical forest. This is a problem for some MEMS, because many devices require features and gaps with a high level of precision to function properly. Because of this, there are two competing objectives that need to be met; the forests need to be straight vertically, and the edges need to be well-defined. The purpose of the second set of experiments is to observe the edge definition of samples grown using iron thicknesses that produce relatively straight forests.

In addition to these findings, the experiment yielded other interesting results. CNT forest straightness is affected by the interaction between iron thickness, feature geometry, and proximity to other features. Features that are in close proximity to other features grow straighter than those that are not. Features on the edge of a device grew differently from features in the center of a device.

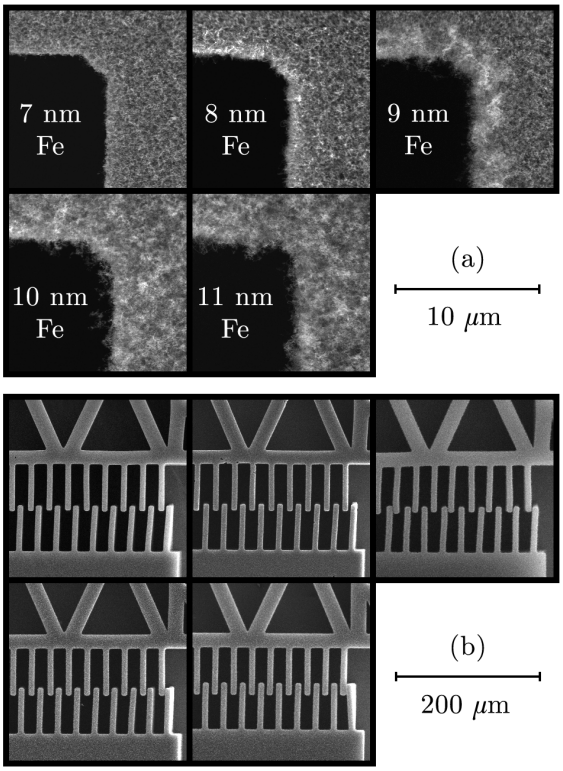

Figure 7. Samples from the second set of experiments. (a) Close-up images of a hole feature show typical edge definition for each sample. Edge definition deteriorates quickly at iron thicknesses above 8 nm. (b) Comb-drive mechanism corresponding to each sample shown in (a). In this range of iron thickness, there does not appear to be any difference in CNT forest straightness.

The effect was more pronounced with very thin layers of iron. This effect is seen in Figure 6, which shows CNT forests all made from the same pattern. Notice that the sample grown with 2 nm of iron has a thin (5 μm) edge feature that did not grow to the same height as the rest of forest. The 4th beam in from the edge is also 5 μm wide, but reached the same height as the rest of the forest. The difference between the thin edge feature and the thin central feature is that the thin central feature has other features in close proximity on all sides. For the same reason, the more bulky portion of the forest (the wide "post" to which all of the beams are connected) grew taller than the rest of the edge. Notice also that the corner of the post is curved, indicating that the side did not grow straight. These effects are barely noticeable in the sample grown with 4 nm iron, and are not noticeable in the sample grown with 7.5 nm iron. As will be discussed later in this paper, it appears that the local availability of iron for pyrolysis has an effect on growth rate, and that iron availability is determined by both the amount of iron deposited, and the proximity of the feature to other regions of iron.

Figure 7 contains a series of SEM images typical of the second set of experiments. Figure 7a shows close-up views of hole features on each sample (7, 8, 9, 10, and 11 nm of iron). As iron catalyst thickness increases from 7 to 11 nm, edge definition deteriorates. Above 9 nm of iron, the nanotubes are much more coarse, produce larger sidewall roughness, and have relatively poor edge definition. Iron thickness does not seem to have an effect on forest straightness in this region, but there appear to be other factors contributing to non-straight growth that are not yet under

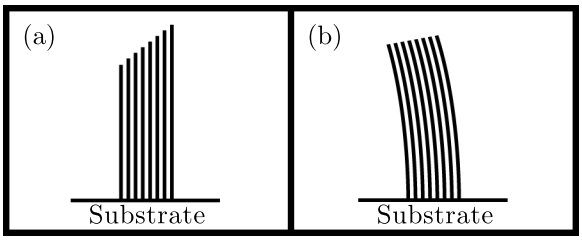

Figure 8. (a) A diagram showing what a feature would look like if well-aligned nanotubes had different growth rates, but did not interact with each other. (b) A diagram showing what well-aligned nanotubes that had different growth rates actually look like, presumably due to interactions between the nanotubes.

control. Figure 7b shows a portion of a comb-drive mechanism corresponding to each sample. These comb-drive mechanisms are 100 μm tall. At this height, there is still some non-straightness in thin features such as the comb-drive fingers. However, this non-straightness appears to be random, and not affected by iron thickness within this range. Based on these results, the ideal range of iron thickness appears to be between 7 and 8 nm, because it yields both relatively straight growth and relatively crisp edge definition. There may be other reasons to choose a different iron thickness in this range. For example, we do not yet know what iron thicknesses produce forests that are ideal for chemical vapor infiltration of various materials.

4. Discussion

In this section, we offer several hypotheses to explain the effect of iron availability on straightness of CNT-MEMS growth.

It appears that some non-straight growth is caused by differences in growth rates across the forest. Consider a hypothetical forest made of nanotubes that were able to grow straight up without interacting with nearby nanotubes. Different growth rates across the forest would result in nanotubes achieving different heights, as shown in Figure 8a. In real CNT forests, however, van der Waals forces prevent fast growing nanotubes from growing much taller than slow growing nanotubes. For samples grown on relatively thin iron layers, the nanotubes stay well-aligned but the forests are non-straight, as shown in Figure 8b. The effect is similar to extruding metal through an asymmetric die, where unequal exit velocities cause the billet to be curved [18].

Now consider the device illustrated in Figure 9a. This device consists of two bulky regions connected by four narrow beams. Just like the edge features in Figure 6, the four narrow beams do not grow as fast as the bulky regions. Intertwining and van der Waals interactions prevent the bulky regions from growing much taller than the beams. As a result, bulky regions are pulled inward, as illustrated in Figure 9b. Suppose that the length of the narrow beams was designed to be 200 μm long, and that the distance between bulky regions at the top of the forest is only 150 μm. The carbon nanotube beams that would have spanned a 200 μm gap are now forced to grow in a tighter space, and as a result, the beams grow outward. This effect may explain the non-straight growth shown in Figure 2.

For samples grown on relatively thick iron layers, van der Waals forces cause nanotubes to intertwine, but the forest as a whole tends to be more straight. The higher level of intertwining

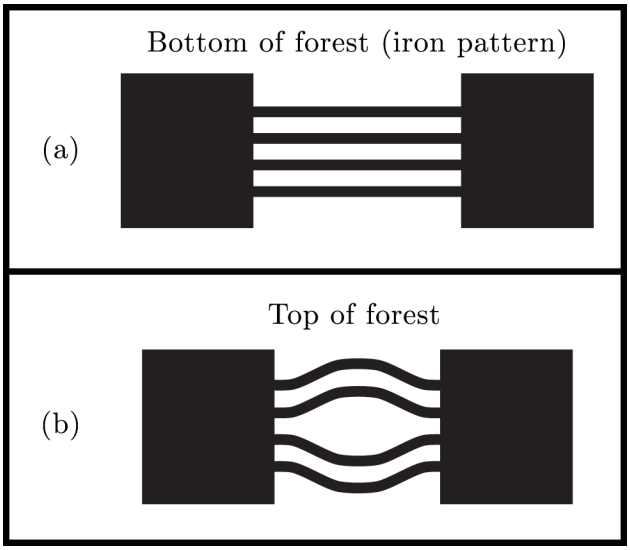

Figure 9. (a) A diagram showing a device in the way it might be patterned onto the wafer. The base of the CNT forest will take on this pattern.(b) A diagram showing the top of the CNT forest for this device. The bulky sides are pulled in towards the center, forcing the narrow beams to grow nonstraight.

has to do with defects in the crystalline nanotube structure. As mentioned previously, thicker iron layers yield higher diameter nanotubes. Higher diameter nanotubes have lower strain energies and therefore more opportunities for defects [19]. These defects cause nanotubes to bend and kink as they grow, which allows for the higher degree of intertwining. Similarly, for thinner iron layers, the higher strain energy associated with smaller diameter nanotubes prevents defects, and therefore prevents kinking. Instead, the entire forest is forced to bend as it grows.

Growth rate depends heavily on iron availability. Figure 10 shows typical growth rates of carbon nanotubes for different iron thicknesses used. For samples with less than 5 nm iron, growth rates are more sensitive to small changes in iron availability than for samples with more than 5 nm iron. For example, the growth rate for 3 nm iron is approximately 50% higher than the growth rate for 2 nm iron, while the growth rates for 7 nm and 10 nm differ by less than 10%. In other words, for thinner iron layers, depositing just a few more atoms of iron on one side of a feature than on the other could lead to very different growth rates across the feature.

Iron availability is determined by both the thickness of iron deposited during fabrication, and the proximity of a feature to other nearby regions of iron. The effect of iron thickness on CNT growth rate suggests that iron plays a role in ethylene decomposition. The ideal gas species for CNT growth are not known; however, polycyclic aromatic hydrocarbons have been proposed as essential for high quality CNT growth [20]. For thin, edge, or sparse features, the gas composition must be different from that in thick, central, or abundant features. We hypothesize that increasing iron thickness mitigates this difference because it provides more local catalyst for the decomposition of ethylene. A similar hypothesis has been proposed to explain the effects of iron pattern density on nanotube growth [9]. As suggested by Figure 6, the reduction in growth variation may also be gained by use of iron borders placed around the outside of thin or edge features.

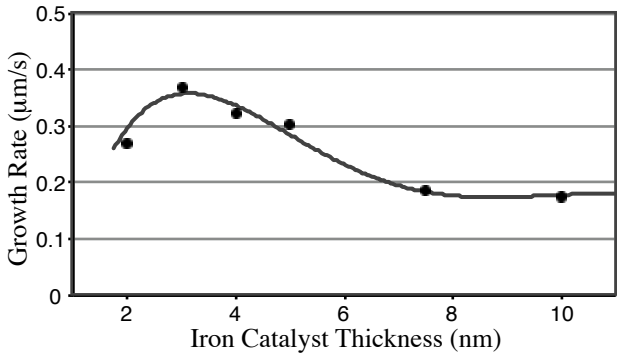

Figure 10. Relative growth rates of carbon nanotubes grown for five minutes. Growth rates for very thin iron layers are more sensitive to small changes in iron availability. The trend line comes from a least squares fit polynomial and is present to help guide the eye.

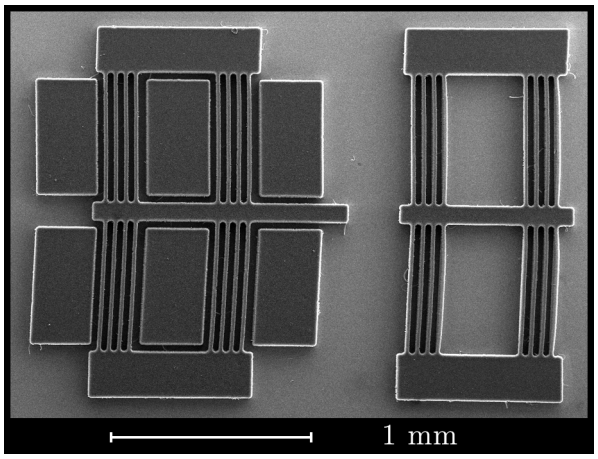

Figure 11. 2 TIMs, one with iron borders and one without. The iron borders are present to promote straight growth. In order to accommodate these borders, the shuttle of the TIM on the left has been extended.

5. Application of Iron Borders

CNT-M designers can take advantage of the fact that central features tend to grow more straight than edge features. Photolithography masks can be designed so that iron is not only where the device will be, but also in the nearby regions surrounding features that are at risk for non-straight growth. In some cases, the device may need to be redesigned to allow for this.

For example, Figure 11 shows two thermomechanical in-plane microactuators (TIMs) [21, 22]. Running a current across the thin legs of these devices causes them to heat up and expand, pushing the shuttle forward, which is toward the right in Figure 11. The TIM on the right is the classic design used with other MEMS fabrication methods. The TIM on the left is surrounded by iron borders, so that the thin legs are more likely to grow straight. To accommodate these iron borders, the shuttle on the left had to be extended in order to still be useful as an actuator.

Figure 12 shows that the iron borders do in fact improve straightness of growth. This is most apparent in the lowest leg in Figure 12. These images are typical of all sets of legs on the TIMs. The post comparison shown in Fig. 13 also illustrates the benefits of posts. The post on the left, with

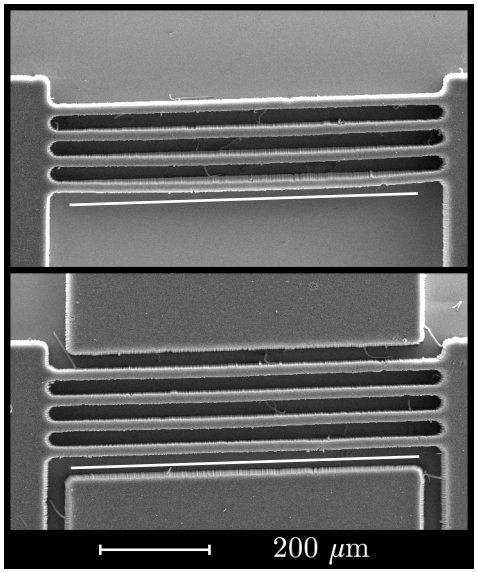

Figure 12. Adding iron borders improves device straightness. Notice the lowest leg for each device; the legs on the device with iron borders are more straight. A straight white line has been added to each image to guide the eye.

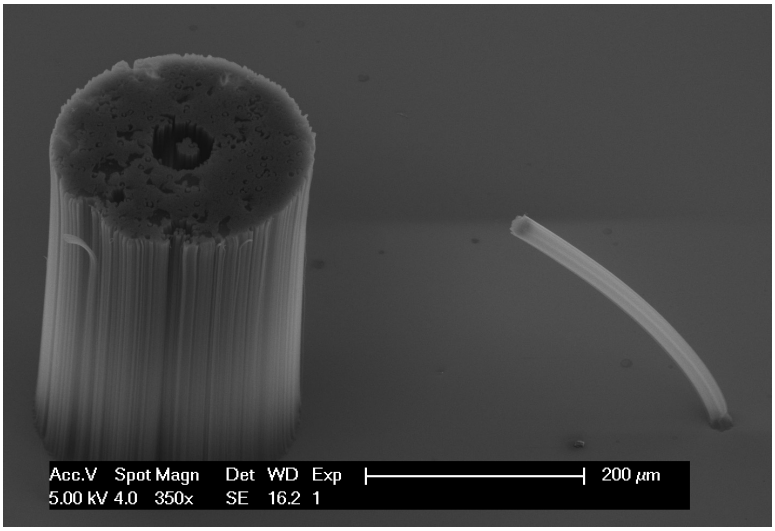

Figure 13. Providing an iron border allowed this 20 μm diameter post in the center to grow straight up to 312 μm; compare the post on the right with the same dimensions and no border.

a border, remained inside the border as it grew. In comparison, the post on the right, without a border, did not grow straight. This technique has been used to create the free-standing post shown in Fig.14. For this image, the carbon nanotubes in the border region were removed manually using tweezers.

6. Conclusions

This paper shows the effect of iron availability on carbon nanotube forest straightness for CNT-M. The straightness of samples fabricated with different iron thicknesses were compared to find an

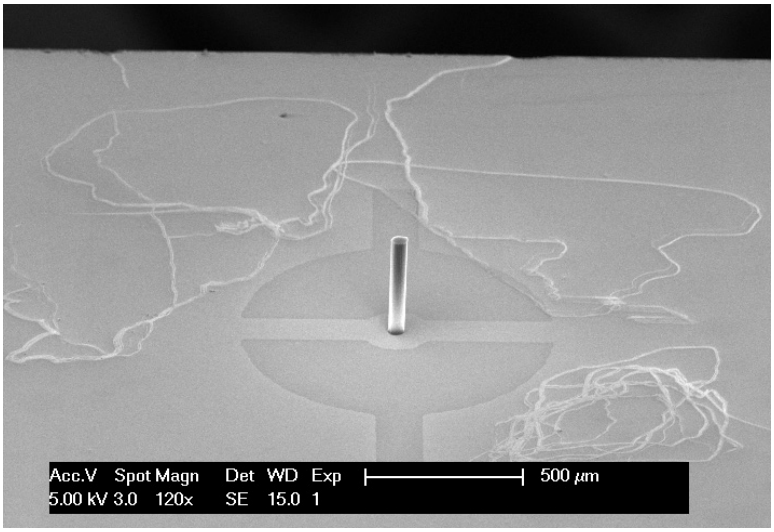

Figure 14. This post with diameter 56 μm grew to a height of 382 μm with a border. The nanotubes in the border region (the dark semicircles around the post) were removed with tweezers.

appropriate range of iron thicknesses for fabricating straight CNT-M devices. The concept of using iron borders to improve device straightness was successfully implemented.

This research offers a hypothesis to explain this behavior. Iron availability is affected by the thickness of iron deposited during fabrication, and by the proximity of a feature to nearby iron. This iron available for pyrolysis affects the local density of the species of ethylene present during CNT growth. Therefore, thin, edge, or sparse features will grow differently than thick, central, or abundant features.

Iron catalyst thicknesses between 7 and 11 nm produce straighter forests than thicknesses below 5 nm. Within the range of 7 to 11 nm of iron, less iron will yield better edge definition. Using different thicknesses within this range may affect compatibility with the material used in chemical vapor infiltration of these forests.

In addition to controlling iron thickness, designers should include an iron border to surround the entire device when possible. This will increase iron availability for edge features and cause them to grow more like central features. When necessary, the device will need to be redesigned in order to accommodate these iron borders.

[1] David N. Hutchison, Nicholas B. Morrill, Quentin Aten, Brendan W. Turner, Brian D. Jensen, Larry L. Howell, Richard R. Vanfleet, and Robert C. Davis. Carbon nanotubes as a framework for high-aspect-ratio mems fabrication. *Journal of Microelectromechanical Systems*, 19(1), February 2010.

[2] DN Hutchison, Q. Aten, B. Turner, N. Morrill, LL Howell, BD Jensen, RC Davis, and RR Vanfleet. High aspect ratio microelectromechanical systems: A versatile approach using carbon nanotubes as a framework. In *Solid-State Sensors, Actuators and Microsystems Conference, 2009. TRANSDUCERS 2009. International*, pages 1604–1607. IEEE, 2009.

[3] Jun Song, David S. Jensen, David N. Hutchison, Brendan Turner, Taylor Wood, Andrew Dadson, Michael A. Vail, Matthew R. Linford, Richard R. Vanfleet, and Robert C. Davis. Carbon-Nanotube-Templated Microfabrication of Porous Silicon-Carbon Materials with Application to Chemical Separations. *Advanced Function Materials*, 21(6):1132–1139, 2011.

[4] W. Ehrfeld, P. Bley, F. Gotz, P. Hagmann, A. Maner, J. Mohr, H.O. Moser, D. Munchmeyer, W. Schelb, D. Schmidt, and E.W. Becker. Fabrication of microstructures using the LIGA process. In *Proc. Micro Robots*

and Teleoperators Workshop, Hyannis, MA, USA, 1987.

[5] M. Jose-Yacaman, M. Miki-Yoshida, L. Rendon, and JG Santiesteban. Catalytic growth of carbon microtubules with fullerene structure. *Applied physics letters*, 62(6), 1993.

[6] SB Sinnott, R. Andrews, D. Qian, AM Rao, Z. Mao, EC Dickey, and F. Derbyshire. Model of carbon nanotube growth through chemical vapor deposition. *Chemical Physics Letters*, 315(1-2):25–30, 1999.

[7] S. Fan, M.G. Chapline, N.R. Franklin, T.W. Tombler, A.M. Cassell, and H. Dai. Self-oriented regular arrays of carbon nanotubes and their field emission properties. *Science*, 283(5401):512, 1999.

[8] C.J. Lee, J. Park, and J.A. Yu. Catalyst effect on carbon nanotubes synthesized by thermal chemical vapor deposition. *Chemical Physics Letters*, 360(3-4):250–255, 2002.

[9] Michael J. Bronikowski. CVD growth of carbon nanotube bundle arrays. *Carbon*, 44:2822–2832, 2006.

[10] Goo-Hwan Jeong, Niklas Olofsson, Lena K. L. Falk, and Eleanor E. B. Campbell. Effect of catalyst pattern geometry on the growth of vertically aligned carbon nanotube arrays. *Carbon*, 47:696–704, 2009.

[11] C.L. Cheung, A. Kurtz, H. Park, and C.M. Lieber. Diameter-controlled synthesis of carbon nanotubes. *J. Phys. Chem. B*, 106(10):2429–2433, 2002.

[12] B. Zhao, D.N. Futaba, S. Yasuda, M. Akoshima, T. Yamada, and K. Hata. Exploring advantages of diverse carbon nanotube forests with tailored structures synthesized by supergrowth from engineered catalysts. *ACS nano*, 3(1):108–114, 2008.

[13] Wei-Hung Chiang, Don N. Futaba, Motoo Yumura, and Kenji Hata. Growth control of single-walled, double-walled, and triple-walled carbon nanotube forests by a priori electrical resistance measurement of catalyst films. *Carbon*, 49(13):4368 – 4375, 2011.

[14] A. Gohier, CP Ewels, TM Minea, and MA Djouadi. Carbon nanotube growth mechanism switches from tip-to base-growth with decreasing catalyst particle size. *Carbon*, 46(10):1331–1338, 2008.

[15] SP Patole, PS Alegaonkar, H.C. Shin, and J.B. Yoo. Alignment and wall control of ultra long carbon nanotubes in water assisted chemical vapour deposition. *Journal of Physics D: Applied Physics*, 41:155311, 2008.

[16] Z. Yao, H.W.C. Postma, L. Balents, and C. Dekker. Carbon nanotube intramolecular junctions. *Nature*, 402(6759):273–276, 1999.

[17] L. G. Zhou and San-Qiang Shi. Formation energy of stone-wales defects in carbon nanotubes. *Applied Physics Letters*, 83(6), 2003.

[18] K. Mori, K. Osakada, and H. Yamaguchi. Prediction of curvature of an extruded bar with noncircular cross-section by a 3-D rigid-plastic finite element method. *International Journal of Mechanical Sciences*, 35(10):879–887, 1993.

[19] Hongjie Dai. *Nanotube Growth and Characterization*, volume 80 of *Topics in Applied Physics*. Springer Berlin / Heidelberg, 2001.

[20] Gilbert D. Nessim, Matteo Selta, Desirée L. PLata, Kevin P. O'Brien, A. John Hart, Eric R. Meshot, Christopher M. Reddy, Phillip M. Gschwend, and Carl V. Thompson. Precursor gas chemistry determines the crystalinity of carbon nanotubes synthesized at low temperature. *Carbon*, 49(3):804–810, March 2011.

[21] C. D. Lott, T. W. McLain, J. Harb, and L. L. Howell. Modeling the thermal behavior of a surface-micromachined linear-displacement thermomechanical microactuator. *Sensors and Actuators A: Physical*, 101:239–250, 2002.

[22] J. W. Wittwer, M. S. Baker, and L. L. Howell. Simulation, measurement, and asymmetric buckling of thermal microactuators. *Sensors and Actuators A: Physical*, 128(2):395–401, 2006.